Mobile MIMO Communications in Urban Environments

Tricia J. Willink
Communications Research Centre
3701 Carling Ave., Box 11490, Station H
Ottawa, ON, K2H 8S2
CANADA

email: tricia.willink@crc.ca

ABSTRACT
Multi-input multi-output (MIMO) technology has the potential to provide large increases in spectral efficiency in scattering propagation environments such as urban scenarios. The physical structure of the environment varies a great deal, from urban canyons to intersections, and this has a significant impact on the capability of the radio channel to support MIMO communications. In this paper, measurement results using an 8×8 MIMO sounder in an urban area are reported. Large variations in the channel are observed as the terminal moves, resulting from the changing spatial diversity. The performance of two MIMO technologies is evaluated for these locations, and it is seen that neither takes satisfactory advantage of the diversity. Adaptive MIMO is necessary for mobile urban communications, to achieve increased spectral efficiency when it can be supported.

1 INTRODUCTION

Urban environments, and other types of complex terrain, have traditionally been thought of as challenging with respect to achieving robust, reliable communications. In more recent years, advances in signal processing techniques have led to the realisation that the characteristics that make the environment challenging can be exploited to improve quality of service.

The transmitter and receiver are rarely in line-of-sight, hence the signal arrives at the receiver after being reflected and scattered from objects in the environment, such as vehicles and buildings, and diffracted around large objects. Reflection occurs from objects that are large with respect to the wavelength of the signal, and scattering arises from smaller objects. When the signal is scattered from an object in the environment, a group of wavefronts arrives at the receiver; these individual multipath components are not resolvable, but they have small differences in angle of arrival, phase and delay.

In a complex propagation environment, multiple copies of the transmitted signal are received from different directions, with different amplitudes, phases and delays. Single element antennas have no capability to resolve in the angular, or spatial, domain. Hence, signals arriving from different angles within the same delay resolution interval combine constructively or destructively, depending on their relative phases. The combined received signal is dependent on the precise location of the transmitter, receiver and other objects interacting with the signal wavefronts. When there is relative movement among the transmitter, receiver and objects in the environment, the relative phases of the signal components arriving within each delay resolution interval change, resulting in combined signals that change over time. This phenomenon is called multipath fading.

The main challenge in the design of signal processing strategies for urban communications is to combat multipath fading. Strategies include: interleaving and forward error correction; delay diversity such as direct sequence spread spectrum; and frequency diversity, for example using orthogonal frequency division multiplexing (OFDM).

When multiple element antennas (MEAs) are used at the transmitter and receiver, elements in different positions receive different combinations of the incoming wavefronts. Such systems are called multiple-input multiple-output (MIMO). As the MEAs move, the signals received at each element experience the same multipath fading processes, but the complex amplitudes of the received signals at a given instant are different at each antenna element. Ideally, the fading on these components is uncorrelated, which means that when one element experiences a fading null, there is a high probability that one or more of the other elements do not. Thus, the spatial diversity provided by the MEA gives robustness against fading, which can be exploited to provide a better quality of service (QoS), i.e., a lower error rate and/or a higher data rate.

In practical urban scenarios, it is observed that there is often significant correlation among the fading signals observed at each antenna element. This results in a reduced capability to achieve very low error rates or to support high data rates; however, as will be seen, there are still considerable potential improvements in QoS available using MIMO but achieving these improvements requires a detailed understanding of the channel characteristics.

The objective of this paper is to describe the propagation characteristics of urban environments, illustrated by measurements obtained at the Communications Research Centre, and to discuss their impact on achieving robust, high data rate communications. Background to the principles of MIMO communications is given in Section 2. The measurement system and campaign are discussed in Section 3, and characteristics of the urban MIMO radio channels are described in Section 4. The performance of two types of MIMO signalling techniques is illustrated using the measured data in Section 5, and a discussion of the potential gains and challenges of implementing MIMO radio systems for tactical urban communications is presented in Section 6.

2 MIMO BACKGROUND

MIMO signalling schemes typically assume that the signal bandwidth is narrow enough that it experiences flat-fading. Wider transmission bandwidths are obtained by multiplexing these narrowband signals together using OFDM. The alternative is to use a wideband signal which will experience frequency-selective fading and therefore inter-symbol interference, and apply equalisation, as in [1]. While frequency-selective fading does provide temporal diversity, and hence robustness against fading, there is generally sufficient diversity available from the spatial domain to provide the required robustness. Additional diversity provides diminishing returns, and the need for multi-dimensional equalisation adds cost and complexity. As chip-based fast Fourier transforms are readily available, OFDM is a cost-effective method. If required, additional robustness can be obtained through frequency diversity.

Henceforth, it will be assumed that the signal bandwidth is sufficiently narrow that the channel can be assumed to be flat-fading. The system model for N_t antenna elements in the transmitter array and N_r in the receiver array is then

$$\mathbf{r}(t) = \mathbf{H}(t)\mathbf{x}(t) + \mathbf{n}(t) \tag{1}$$

where $\mathbf{x}(t)$ is the length-N_t transmitted signal vector, and the jth element $x_j(t)$ is transmitted from the jth antenna element. The channel response is given by the $N_r \times N_t$ matrix, $\mathbf{H}(t)$, where the (i, j)th element $H_{ij}(t)$ is the complex response between the jth element of the transmitter array and the ith element of the receiver array. The length-N_r received signal vector $\mathbf{r}(t)$ is the combination of the signal component and the noise vector, $\mathbf{n}(t)$. The N_r elements of $\mathbf{n}(t)$ are assumed to be independent and identically distributed (i.i.d.) complex Gaussian random variables with zero mean and variance σ_n^2.

The potential gain of the MIMO system can be seen by considering its ergodic capacity, which is the amount of information that can be sent through the channel with a negligible probability of error. For a system with a single antenna at the transmitter and receiver, i.e., single-input single-output (SISO), assuming no knowledge of the channel state information at the transmitter, the ergodic capacity per unit bandwidth is

$$C_{SISO}(t) = \mathcal{E}\left\{\log_2\left(1 + \frac{Ph(t)}{\sigma_n^2}\right)\right\} \quad \text{b/s/Hz} \tag{2}$$

where $h(t)$ is the complex channel response, P is the average transmitted power and $\mathcal{E}\{\cdot\}$ denotes expectation.

The equivalent capacity of a MIMO system using the same total average transmitted power is [2]

$$C_{MIMO}(t) = \mathcal{E}\left\{\log_2 \det\left(\mathbf{I} + \frac{P}{N_t\sigma_n^2}\mathbf{H}(t)\mathbf{H}^H(t)\right)\right\} \quad \text{b/s/Hz} \tag{3}$$

where 'det' denotes determinant, and $\cdot^H$ denotes the complex conjugate transpose. The average power transmitted from each of the N_t antennas elements is P/N_t. This capacity can be shown to be equal to

$$C_{MIMO}(t) = \sum_{i=1}^{\min(N_t,N_r)} \mathcal{E}\left\{\log_2\left(1 + \frac{P}{N_t\sigma_n^2}\lambda_i(t)\right)\right\} \quad \text{b/s/Hz} \tag{4}$$

where $\lambda_i(t)$ is the ith eigenvalue of $\mathbf{H}(t)\mathbf{H}^H(t)$.

Early in the history of MIMO communications system analysis [2]–[4], it was assumed that the elements of $\mathbf{H}(t)$ are i.i.d. zero-mean complex Gaussian random variables. This is supported by the isotropic scattering models of Clarke and Aulin [5, Ch. 2], which assume that there is a large number of multipath components, and that they arrive with uniform probability from all directions. As seen by the analysis of spatial correlation for this model [5, Ch. 2], the fading correlation is small when the antennas are spaced by at least one-half wavelength.

With this assumption, the increase in capacity of a MIMO system relative to a SISO system *with the same transmit power* is shown in Fig. 1 for $N_t = N_r$. The ergodic capacity increases linearly with increasing array sizes. The reason for the phenomenal interest in MIMO since the publication of early papers in this area is clear.

More recently, as more research groups have developed the capability to measure real MIMO operating environments, it has been realised that the assumption of uncorrelated fading at each antenna element is often unrealistic. Correlation changes the distribution of the eigenvalues λ_i such that the largest values become larger, while the smaller ones decrease. For a fixed $\sum_i \lambda_i$, i.e., a fixed received signal power, the

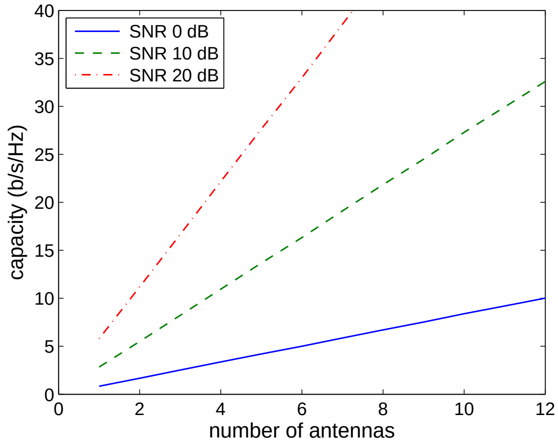

Figure 1: Ergodic capacity for i.i.d. complex Gaussian MIMO channel.

capacity is maximised when the eigenvalues are equal. The impact of correlation is therefore to reduce the capacity.

Some propagation environments may be particularly rich, such as cluttered indoor offices, but in general there is a finite number of multipath components, which reduces the capacity [6]. Furthermore, the physical environment often limits the distribution of angles of departure and arrival of the multipath components. This is illustrated in Fig. 2, which shows urban streets with buildings (grey) and simplified propagation paths. The transmitter is located at 'TX' and the receiver moves along the street from 'A' to 'C'. At receiver location 'A', the signal arrives from many different directions, leading to a high diversity and channel capacity. Between 'A' and 'B' there is good signal power, because multipath components arrive from the junction as well as through the space between the buildings. However, if the distance 'A' to 'B' is large, the angles of arrival would be limited and the angular spread would be limited because the main sources of reflection and scattering are the buildings on each side of the street. This would lead to correlation at the receiver array, and hence a reduced capacity. At receiver location 'C', all the signal energy is being received along the urban canyon, including the component diffracted at the corner 'D'. Not only is the received power low, but the angular spread and hence diversity is small. In this location, the main advantage spatial processing offers is the array gain obtained from beamforming.

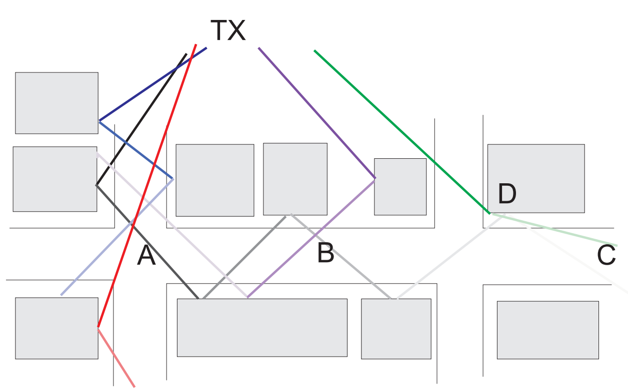

Figure 2: Illustration of spatial diversity in an urban environment.

3 MIMO MEASUREMENTS

It is clear from the foregoing discussion that measurements in real operating environments are essential to understanding the true potential of MIMO signal processing. The Communications Research Centre has developed a wideband MIMO sounder, which has been used to obtain channel measurements in a variety of environments. The sounder and data processing are outlined below, and the measurement locations are described.

Sounder

The CRC MIMO radio channel sounder supports up to eight elements in each of the transmitter and receiver arrays. The 25 MHz bandwidth signals transmitted from each element are continuously repeated binary pseudo-noise (PN) sequences, BPSK-modulating carriers at approximately 2 GHz. The PN sequences were selected in such a way that the impulse responses corresponding to each of the transmitter elements could be readily extracted and identified at the receiver.

Each antenna element at the receiver terminal has its own RF chain, frequency and phase synchronised with the others. The signals received at each element are sampled simultaneously at 50 Msamp/s, and the channel response is sampled at 250 Hz, which is more than twice the maximum Doppler frequency. A technical description of the MIMO sounder is given in [7].

The sampled signals are recorded for off-line data processing, which involves computing and separating the impulse response estimates (IREs) for each of the $N_t \cdot N_r$ links. A threshold was applied to each IRE to reduce the noise; the threshold was computed to provide a lower probability of false alarm. Each IRE was Fourier transformed, and a single spectral line was extracted to provide the complex channel gain of a narrowband channel, $\tilde{\mathbf{H}}(k)$.

A power correction was applied to the data series to reduce the impact of path loss and shadowing. This was done by normalising each measured channel response matrix, $\tilde{\mathbf{H}}(k)$, using a running window, yielding the power-corrected channel matrix

$$\mathbf{H}(k) = \frac{\tilde{\mathbf{H}}(k)}{\left[\frac{1}{N_r N_t K}\sum_{n=k-K/2}^{k+K/2-1} \|\mathbf{H}(n)\|_F^2\right]^{\frac{1}{2}}} \tag{5}$$

where $\|\mathbf{H}\|_F = \left[\sum_{i=1}^{N_r}\sum_{j=1}^{N_t} |H_{ij}|^2\right]^{\frac{1}{2}}$ is the Frobenius norm; H_{ij} is the (i, j)th element of $\mathbf{H}$.

Measurement campaign

The data used in the analyses presented herein were collected with arrays consisting of eight quarter wavelength monopole antenna elements, arranged linearly and spaced by one-half wavelength. The transmitter was static, located approximately 15 m above street level in the centre of a large window oriented at $45°$ to the street, as shown in Fig. 3. The receive antenna array was mounted on the roof of a van.

The receiver terminal was driven along the streets marked in Fig. 3, at approximately 30 km/h. The measurements were made on the weekend, when the traffic volume and density of parked cars in the downtown core were minimal.

The four measurement routes shown in Fig. 3 are non-line-of-sight (NLOS), but have different characteristics. The route along Slater is in the same urban canyon as the transmitter, and the building façades are uniform. The number and angular spread of the dominant multipath components at the receiver are quite small. Laurier runs parallel to Slater, hence most of the signal energy is received by diffraction and/or reflection between the two blocks, and the spatial diversity is expected to be higher, although the unnormalised received power is lower. Kent and Bank run perpendicular to Slater, hence the signal energy is also received due to diffraction and/or reflection. The route along Bank crosses Slater, at which point there is expected to be a strong component from the direction of the transmitter, which will reduce the spatial diversity in the intersection; at this point, the unnormalised received power will be higher, resulting in a net gain in capacity if power control is not applied. The route on Kent does not cross Slater, thus the characteristics are expected to be more similar to those on Laurier.

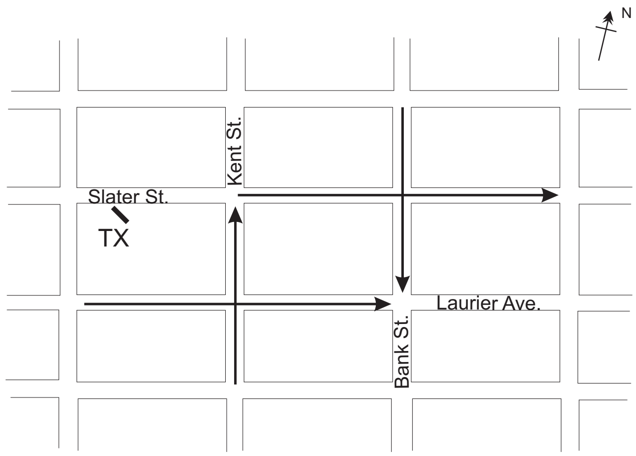

Figure 3: **Map of measurement campaign in urban Ottawa.**

4 MEASURED CHANNEL CHARACTERISTICS

The motivation for using MIMO communications is to increase the spectral efficiency. The first concern, then, with the measurements is to evaluate the increase in capacity relative to single antenna measurements. An important feature of mobile urban environments is the dependence of the channel characteristics on location. As the mobile receiver moves from one location to another, the correlation and hence also the capacity change.

4.1 Capacity

The usual metric used to evaluate MIMO channels is the Shannon capacity, given in (4). Empirical cumulative distribution functions (cdfs) of the capacity computed over the length of the routes in Fig. 3 are shown in Fig. 4. Different array sizes ($N_r = N_t = 1$, $N_r = N_t = 2$, $N_r = N_t = 4$ and $N_r = N_t = 8$) have been used, each with antenna spacing one-half wavelength. The capacity for the ‘ideal’ channel, with i.i.d. complex Gaussian elements in $\mathbf{H}(n)$ is also plotted. For the SISO (1×1) case, capacity of the measured channels is very close to that of the ideal channel, because the power normalisation (5) has removed the advantage of the specular (Ricean) components. As noted above, Slater has the highest spatial correlation – this results in the lowest capacity. Note also that the difference increases as the size of the array increases. On Slater, most of the power is carried in a small number of multipath components

– increasing the array aperture in this case does not increase the diversity to the same degree it does on Laurier, which has lower correlation reflecting a more uniform distribution of power among the multipath components. However, none of the measurements provides the same capacity as the ideal channel model. In spite of this, it is clear that the capacity increases significantly as the array size increases.

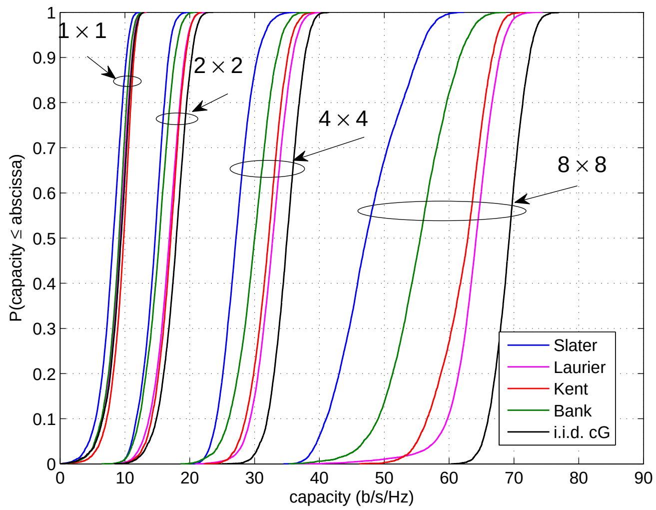

Figure 4: **Cdfs of capacity for measured and simulated data at 30 dB.**

4.2 Time-variation

The cdf of capacity in Fig. 4 shows that a range of capacity values is observed on each of the routes. The dependence of the capacity on location is important for considering adaptive MIMO systems. Fig. 5 shows the variations of capacity over time at 30 dB for the four routes. The capacity has been smoothed using a ten tap Blackman-Harris window (ten taps = 0.08 ms) to remove the rapid fading effects.

After power-correction, the capacity on Laurier is the most uniform. From Fig. 3, it can be seen that Laurier runs parallel to Slater, which is the urban canyon in which the transmitter is located. The high capacity observed is due to a high degree of scattering, which is also responsible for the rapid changes seen even after smoothing. Large variations in the capacity are observed only near the start and end of the measurement run, when the receiver is at an intersection. Small changes in the capacity are also observed between 4 and 6 s, when the vehicle is passing through the intersection with Kent. This intersection has a large open area to the west, which means the sharp changes observed at the intersections with Lyon and Bank are not seen here. In contrast, there is a significant reduction in capacity when the receiver crosses Slater – at this point, there is a very dominant multipath component arriving along Slater which reduces the spatial diversity and hence the capacity. A similar effect is observed at the end of the route on Kent. The variation in capacity is largest along Slater. In this case, the received signal is dominated by one or more multipath components travelling along Slater, i.e., with a small angular spread, resulting in a smaller capacity than measured on the other streets. The capacity then depends on the number and strength of these components, which varies as the vehicle moves along the street.

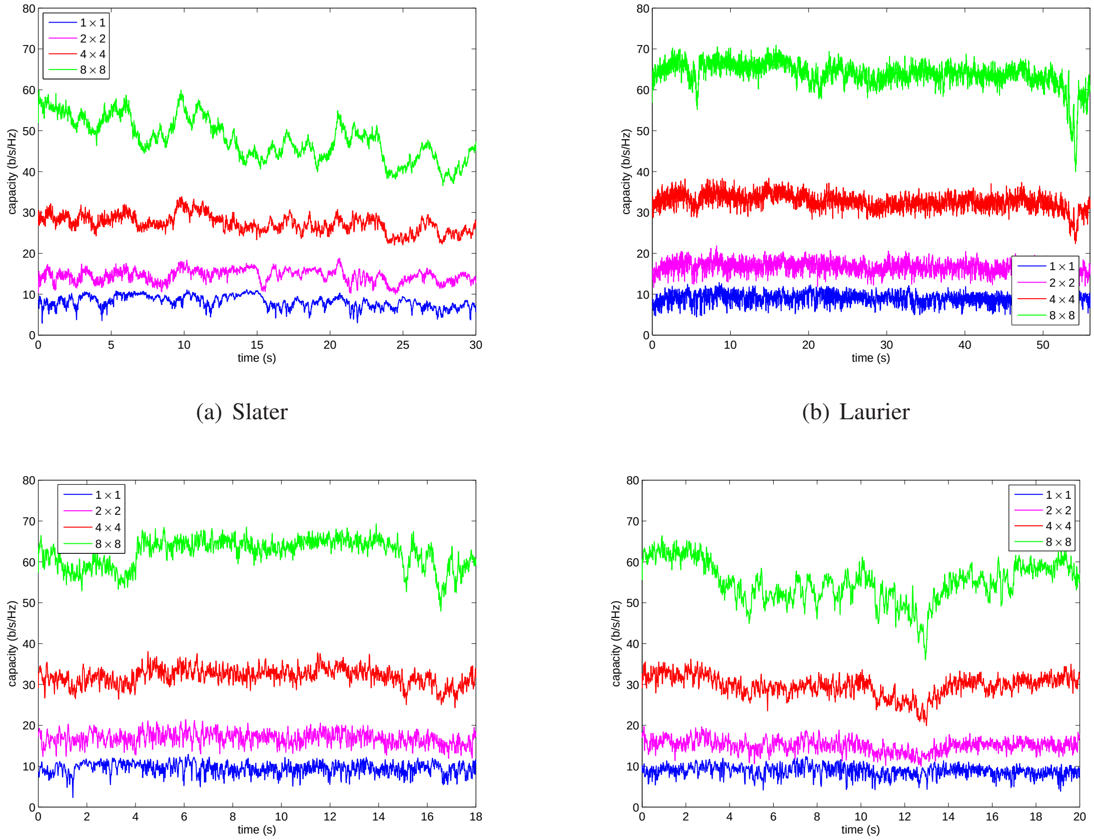

(a) Slater (b) Laurier

(c) Kent (d) Bank

Figure 5: **Time-varying capacity for measured data at 30 dB.**

An important feature of mobile communications, which is often overlooked in evaluating channel characteristics, is that the time-series of channel responses is generally nonstationary. Recent results presented in [8] show that typically less than 10% of one-half second intervals can be assumed to be wide-sense stationary.

5 SYSTEM PERFORMANCE

The impact of location on performance is illustrated using two MIMO signal processing techniques: space-time coding and spatial multiplexing. Space-time coding, in this case, block coding, is used to exploit the spatial diversity in the channel to improve bit error rate (BER) but does not increase the throughput; thus, the rate is one. Spatial multiplexing uses the spatial diversity to support an increase in the number of paths, generally increasing the throughput by a factor N_t.

The two signal processing techniques will be evaluated for $N_t = N_r = 4$ antenna elements, using the power-corrected channel measurements discussed above. QPSK modulation is used for each technique, and it is assumed that the receiver has perfect channel state information in both cases. No channel state information is available at the transmitter.

5.1 Space-time block coding

For this example, a four-dimensional *quasi-orthogonal* space-time block code (STBC) was used. This code achieves a diversity gain of $2N_r$: an ideal STBC for $N_t = 4$ would achieve a diversity gain of $4N_r$, however there are no such full-rate (i.e., rate one) complex codes for $N_t > 2$. When all $N_r = 4$ are used, the loss in diversity gain is relatively small. Four consecutive complex data symbols, s_1, s_2, s_3 and s_4 are transmitted in four consecutive symbol intervals using the code given by [9]

$$\mathbf{X} = \begin{bmatrix} s_1 & -s_2^* & -s_3^* & s_4 \\ s_2 & s_1^* & -s_4^* & -s_3^* \\ s_3 & -s_4^* & s_1^* & -s_2 \\ s_4 & s_3^* & s_2^* & s_1 \end{bmatrix}. \tag{6}$$

Note that each symbol, s_i, $i = 1, \ldots, 4$ is transmitted once during each time interval, and once from each transmitter element. This ensures that each symbol has the same reliability in detection. The transmitted symbols are detected using a maximum-likelihood (ML) technique, as described in [9].

5.2 Spatial multiplexing

Increased throughput is achieved by transmitting parallel independent data substreams simultaneously from each of the transmitter elements with equal power. At the receiver, these substreams interfere with each other, and nonlinear spatial processing is required to extract the transmitted symbols unless $N_r \gg N_t$. A simple, but computationally complex, successive interference cancellation (SIC) scheme was proposed in [10], [11]. This scheme is called V-BLAST, for vertical Bell-Labs layered space-time architecture. The strongest signal is detected first using linear spatial processing, then its contribution to the received signal vector is cancelled. The second strongest signal is then detected in a similar way. Thus, error propagation is minimised, but not eliminated, by detecting the strongest signal at each step, i.e., that which is least likely to be in error.

5.3 Performance

The bit error rates for the quasi-orthogonal STBC and for spatial-multiplexing using V-BLAST are shown in Fig. 6. The SNR was 6 dB for the STBC (QOST) and 12 dB for the spatial multiplexing. The impact of the changing spatial diversity can be clearly seen in the rapidly varying performance. At these SNRs, the performance of the two schemes is similar on Laurier, which was seen in Fig. 4 to have the highest capacity. On Slater, which has the lowest capacity, the spatial multiplexing fails to achieve a practical BER. While the STBC provides reasonable performance most of the time, it is highly variable. Note that between 4 and 5 s, when the capacity increases, the BER is worst. This indicates that the capacity is driven by a single strong multipath component, effectively producing conditions similar to line-of-sight, in which the capacity is high but the spatial diversity is low. The BER performance of STBC reflects this low diversity. The BER performance of the two techniques on Kent and Bank is also rapidly varying, dependent on the location of the receiver.

These results illustrate the problems of systems confined by rate. Recall that the rate of the STBC is $r_{QOST} = 1$, while the rate of the spatial multiplexing is $r_{VBLAST} = N_t$. To fully utilise the potential of the spatial diversity, while maintaining an acceptable performance, it is necessary to have a range of rates available, bridging the gap between conventional space-time coding and spatial-multiplexing.

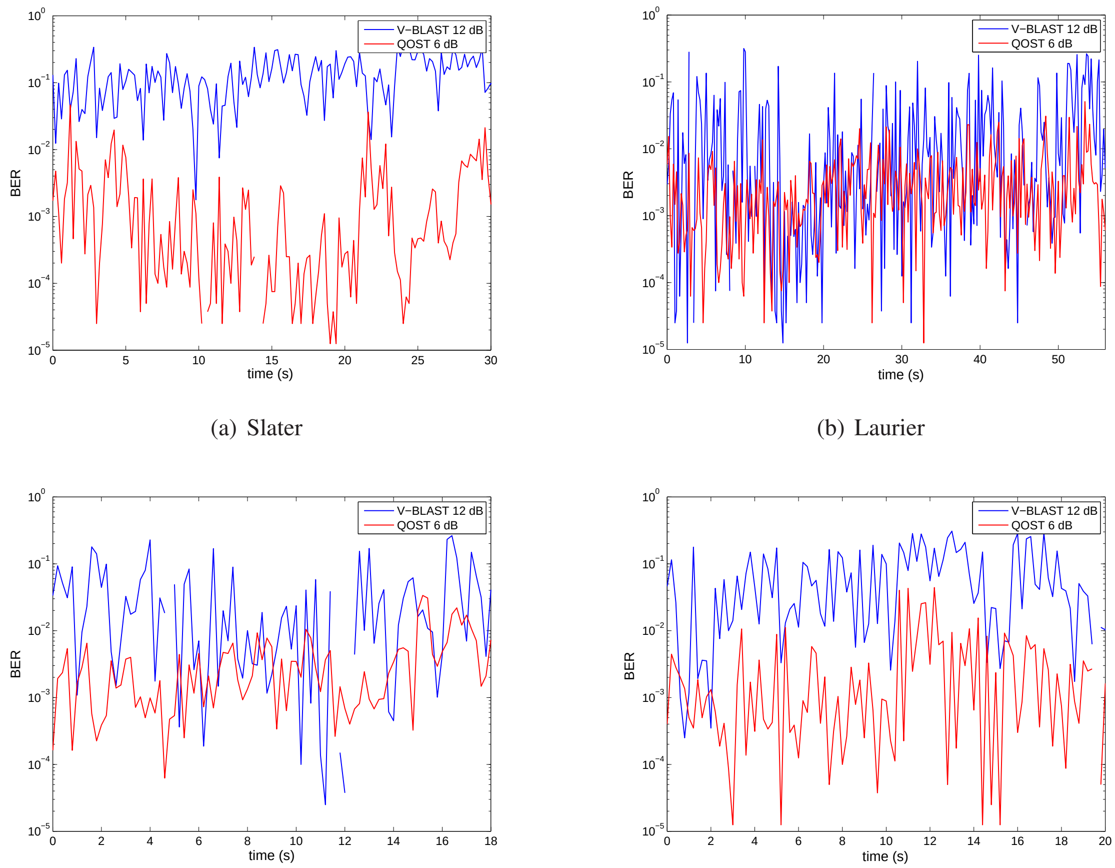

(a) Slater (b) Laurier

(c) Kent (d) Bank

Figure 6: **Performance of STBC and V-BLAST using measured data. SNR is 6 dB for STBC and 12 dB for V-BLAST.**

6 DISCUSSION

MIMO communications technology has considerable potential to increase the spectral efficiency in scattering environments, such as urban tactical scenarios. Although the gains are not as high as predicted by the early, optimistic spatially-uncorrelated models, the spectral efficiency increases almost linearly with the number of antenna elements for practical array sizes.

An important feature of the urban environment is mobility, either of the terminals or of the objects that interact with the wavefronts. This mobility changes the spatial pattern of the multipath components, which in turn varies the spatial diversity of the channel. In urban canyons, where the signal energy is dominantly arriving from the front and rear of the vehicle, the diversity is low. As the vehicle moves through this environment, the changes in diversity can be quite rapid. When signal energy arrives more uniformly from a wider angular range, the diversity increases.

The rapid and large changes in diversity are reflected in the MIMO channel capacity, and in the performance for different MIMO signalling techniques. When the diversity is low, the channel cannot support the high-rate spatial multiplexing, but when the diversity is high, space-time codes provide very low error rates but no increase in throughput.

It is clear that there is a requirement for variable rate capability, allowing the radio to take advantage of high diversity to achieve a high throughput at a reasonable error rate. When the diversity is reduced, the radio must reduce its throughput to achieve the required error rate. Without adaptivity, the system will most likely be operating in the lowest data rate mode, which is the only way that the required error performance can be guaranteed. This wastes much of the MIMO potential. This type of adaptivity requires that the transmitter has some information about the state of the channel, requiring a feedback link.

Signalling techniques to provide these variable rates have been proposed. Two examples are the limited feedback precoding (LFP) introduced in [12], [13] and orthogonal diversity-multiplexing precoding (ODMP) proposed in [14]. The range of rates provided by ODMP is shown in Fig. 7 for a 4×4 MIMO system. The BER extremes are achieved by the rate-1 STBC and the rate-4 spatial multiplexing. The ODMP provides rates $\{1, 1.5, 2, 3\}$ which bridge the gap between these extremes.

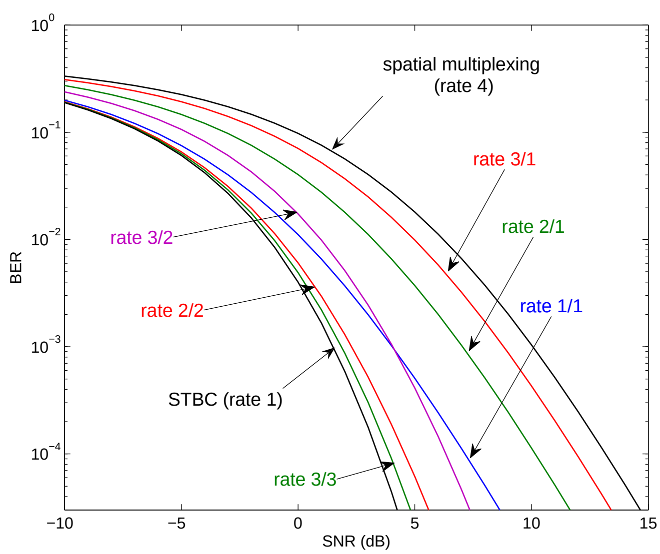

Figure 7: BER for ODMP variable-rate precoding for 4×4 MIMO [14].

The two variable rate precoding methods, LFP and ODMP, both have very low feedback requirements: in LFP the index of the codeword best suited to the channel matrix $\mathbf{H}(k)$ is fed back, and in ODMP, the code rate is fed back. The LFP techniques was evaluated using measured data in [15], and the impact of imperfect channel estimation, resulting from noise, time-variation in the channel and delays in the feedback, was also considered.

The spatial channel structure, i.e., the number, direction and relative strength of the multipath components, changes rapidly as the terminal moves, even at relatively low speeds. This means that the MIMO system must be able to adapt rapidly to achieve robust communications at the required QoS. Such sophisticated signal processing must be supported by advanced adaptive strategies, requiring cross PHY/MAC layer implementations. Without these capabilities, MIMO will not fulfil its potential to increase spectral efficiency.

Acknowledgements

This work was supported by Defence R&D Canada. Thanks to Chris Squires and Geoff Colman for their measurement and data analysis support.

References

[1] Y. L. C. de Jong and T. J. Willink, "Reduced-complexity time-domain equalization for turbo-MIMO systems," *IEEE Trans. Commun.*, vol. 55, pp. 1878–1883, Oct. 2007.

[2] E. Telatar, "Capacity of multi-antenna Gaussian channels," vol. 10, pp. 585–595, Nov.-Dec. 1999.

[3] J. Winters, "On the capacity of radio communication systems with diversity in a Rayleigh fading environment," *IEEE J. Select. Areas Commun.*, vol. 5, pp. 871–878, June 1987.

[4] G. Foschini and M. Gans, "On the limits of wireless communications in a fading environment when using multiple antennas," *Wireless Personal Commun.*, vol. 6, Mar. 1998.

[5] G. Stüber, *Principles of mobile communication*. Norwell, MA.: Kluwer, 1996.

[6] A. G. Burr, "Capacity bounds and estimates for the finite scatterers MIMO wireless channel," *IEEE J. Select. Areas Commun.*, vol. 21, pp. 812–818, June 2003.

[7] C. Squires, T. Willink, and B. Gagnon, "A flexible platform for MIMO channel characterization and system evaluation," in *WIRELESS 2003 - Proc. 15th Conf. on Wireless Commun.*, (Calgary, Canada), July 2003.

[8] T. J. Willink, "Wide-sense stationarity of mobile MIMO radio channels," *IEEE Trans. Veh. Technol.*, Mar. 2008.

[9] H. Jafarkhani, "A quasi-orthogonal space-time block code," *IEEE Trans. Commun.*, vol. 49, pp. 1–4, Jan. 2001.

[10] P. W. Wolniansky, G. J. Foschini, G. D. Golden, and R. A. Valenzuela, "V-BLAST: an architecture for realizing very high data rates over the rich-scattering wireless channel," in *1998 URSI Int. Symp. on Signals, Systems, and Electronics, 1998*, pp. 295–300, Sept. 1998.

[11] G. D. Golden, G. J. Foschini, R. A. Valenzuela, and P. W. Wolniansky, "Detection algorithm and initial laboratory results using V-BLAST space-time communication architecture," *Elect. Lett.*, vol. 35, Jan. 1999.

[12] D. Love and R. Heath, "Multimode precoding for MIMO wireless systems," *IEEE Trans. Signal Processing*, vol. 53, pp. 3674–3687, Oct. 2005.

[13] D. Love and R. Heath, "Limited feedback unitary precoding for spatial multiplexing systems," *IEEE Trans. Inform. Theory*, vol. 51, pp. 2967–2976, Aug. 2005.

[14] G. W. K. Colman and T. J. Willink, "Orthonormal diversity-multiplexing precoding in MIMO systems at finite SNR," *IEEE Commun. Lett.*, vol. 11, pp. 650–652, Aug. 2007.

[15] G. W. K. Colman and T. J. Willink, "Limited feedback precoding in realistic MIMO channel conditions," in *Proc. ICC 2007*, pp. 4363–4368, Sept. 2007.